

$$k_1/(k_8[I] + k_1 + [\text{Be}]k_{10}) = 225 \text{ l. mol}^{-1}$$

If we neglect<sup>24-26</sup> the  $k_9 + [\text{Be}]k_{10}$  term in eq 13, and since  $[I] = 2.20 \pm 0.1 \times 10^{-4} \text{ mol l.}^{-1}$ , a minimum value for  $k_8/k_7$  is 20. This very interesting piece of information shows that the quenching rate constant  $k_8$  is one of the largest measured for quenching of benzenoid triplets by organic molecules. Lee and Haninger<sup>28</sup> and Morikawa and Cvetanović<sup>27</sup> have obtained values of 14 and 16, respectively, for  $k_q/k_7$ , where  $k_q$  is the

quenching rate constant for quenching by 1,3-butadiene. The value of 20 for  $k_8/k_7$  obtained here implies that triplet energy transfer between benzene derivatives is very efficient.

**Acknowledgment.** The author wishes to thank the Camille and Henry Dreyfus Foundation and the Robert A. Welch Foundation for financial support. The helpful guidance of Professor W. A. Noyes, Jr., and Professor G. J. Fonken is gratefully acknowledged.

## A Molecular Orbital Study of the Low-Energy Electronic States of Ketene

Janet E. Del Bene

Contribution from the Department of Chemistry, Youngstown State University, Youngstown, Ohio 44503. Received September 30, 1971

**Abstract:** *Ab initio* SCF and SCF-CI calculations with a minimal STO-3G basis set have been performed on the low-lying electronic states of ketene. Vertical excitation energies to the  $^3A_2$ ,  $^1A_2$ , and  $^3A_1$  states are calculated. These states are then geometry optimized, and 0-0 transition energies are obtained. The calculated excitation energies are compared with experimental data, and the transitions which give rise to the long wavelength bands in the uv spectrum are identified. The  $A_2$  states are found to arise from  $\pi \rightarrow \pi'^*$  transitions. The lowest triplet state of ketene results from optimization of the  $^3A_1$  state, which arises from a  $\pi \rightarrow \pi^*$  transition. Potential curves for the dissociation of ketene into  $\text{CH}_2$  and CO are also presented and used as a basis for discussion of the photochemistry of this molecule.

The electronic absorption spectrum of ketene has been the subject of investigation by many spectroscopists. Among the first to measure the spectrum of this molecule were Lardy in 1924<sup>1</sup> and Norrish, Crone, and Saltmarsh in 1933.<sup>2</sup> More recently, Dixon and Kirby,<sup>3</sup> Rabalais, McDonald, Scherr, and McGlynn,<sup>4</sup> and Laufer and Keller<sup>5</sup> have recorded and analyzed the spectrum of ketene. Despite these detailed studies the nature of the low-energy excited states of this molecule have not been well characterized. Moreover, there is disagreement among recent studies in so fundamental a question as whether or not the ketene spectrum results only from spin-allowed transitions. Hence, a theoretical study of the geometries and energies of low-lying electronic states of ketene would be of value in answering questions posed by spectroscopic studies of this molecule.

Ketene is also of interest to photochemists, since irradiation of ketene has often been used as a source of both singlet and triplet methylene radicals. Spin conservation rules require that triplet ketene be the precursor of triplet methylene and that singlet ketene be the source of singlet methylene. Undoubtedly, an understanding of the mechanism of photolysis in ketene will be aided by a description of the electronic structures of states involved in photochemical processes.

Recently, *ab initio* self-consistent field (SCF) configuration interaction (CI) calculations have been reported for a rather large group of small molecules.<sup>6,7</sup> These studies have shown that minimal basis calculations can approximate the excitation energies of low-lying molecular electronic states quite well. In those cases where the excited state geometries have been determined experimentally, there was satisfactory agreement between calculated and experimental values for bond angles and bond lengths. It would therefore seem appropriate to carry out *ab initio* calculations on ketene in order to describe the geometries and electronic structures of the low-energy states of this molecule. This paper reports the results of such calculations. An analysis of these results should provide some insight into the spectroscopic and photochemical behavior of ketene.

### Method of Calculation

For a molecule with  $2n$  electrons the closed-shell ground state wave function can be written in the form of a single determinant

$$\Psi = |\psi_1(1)\bar{\psi}_1(2) \dots \psi_n(2n-1)\bar{\psi}_n(2n)| / \sqrt{(2n)!} \equiv |1\bar{1}2\bar{2} \dots n\bar{n}|$$

in which  $n$  orbitals are each occupied by two electrons. A molecular orbital  $\psi_i$  may be expressed as a linear combination of atomic basis functions  $\phi_\mu$  (the LCAO

(1) G. C. Lardy, *J. Chim. Phys.*, **21**, 353 (1924).

(2) R. G. W. Norrish, H. G. Crone, and O. D. Saltmarsh, *J. Chem. Soc.*, 1533 (1933).

(3) R. N. Dixon and G. H. Kirby, *Trans. Faraday Soc.*, **62**, 1406 (1966).

(4) J. W. Rabalais, J. M. McDonald, V. Scherr, and S. P. McGlynn, *Chem. Rev.*, **71**, 73 (1971).

(5) A. H. Laufer and R. A. Keller, *J. Amer. Chem. Soc.*, **93**, 61 (1971).

(6) R. Ditchfield, J. E. Del Bene, and J. A. Pople, *ibid.*, **94**, 703 (1972).

(7) R. Ditchfield, J. E. Del Bene, and J. A. Pople, *ibid.*, in press.

approximation)

$$\psi_i = \sum_{\mu} c_{\mu i} \phi_{\mu}$$

The coefficients  $c_{\mu i}$  are to be determined and this is done in a standard way by solving the Roothaan equations,<sup>8</sup> thereby obtaining a self-consistent wave function for the ground state.

In addition to the orbitals  $\psi_1, \psi_2, \dots, \psi_n$  which are doubly occupied in the ground state, the SCF procedure leads to a set of unoccupied orbitals  $\psi_{n+1}, \psi_{n+2}, \dots$ . These virtual orbitals are useful in describing excited electronic configurations. Thus the promotion of an electron from an occupied orbital  $\psi_i$  to a virtual orbital  $\psi_j$  gives rise to a singlet configuration

$${}^1\Psi_i^j = [ |1\bar{1} \dots i\bar{l} \dots n\bar{n}| - |1\bar{1} \dots \bar{i}l \dots n\bar{n}| ] / \sqrt{2}$$

and to the three components of a triplet

$${}^3\Psi_i^j = \begin{cases} |1\bar{1} \dots i\bar{l} \dots n\bar{n}| \\ |1\bar{1} \dots i\bar{l} \dots n\bar{n}| + |1\bar{1} \dots \bar{i}l \dots n\bar{n}| \\ |1\bar{1} \dots \bar{i}l \dots n\bar{n}| \end{cases} / \sqrt{2}$$

While a single configuration may in some cases approximate an excited electronic state, it does not adequately take into account electron reorganization in that state. To describe this process mathematically, it is necessary to form various singly excited configurations and allow these to interact *via* a configuration interaction calculation. Such a calculation leads to an improved excited state energy and wave function

$$\Phi = \sum_i^{\text{occ}} \sum_l^{\text{unocc}} A_{il} \Psi_i^l$$

where the coefficients  $A_{il}$  are determined by the variational principle. Since it is generally not possible to include all singly excited configurations in the CI expansion, a method was previously proposed for selecting a subset of configurations to be included.<sup>9</sup> This subset consists of all singly excited configurations which can be formed from the  $M$  highest occupied and the  $M$  lowest energy virtual orbitals. In this work, the value of  $M$  is fixed at 6, the number of virtual orbitals resulting from the minimal basis SCF calculation. Hence, at each geometry, the closed shell SCF equations are first solved and then 36 singly excited configurations are formed and allowed to interact to obtain the excited state wave functions. It was shown in ref 9 that this method gives results close to those of a full first-order CI calculation obtained with a minimal basis set.

The basis set  $\phi_{\mu}$  used for the expansion of the molecular orbitals is minimal (1s for hydrogen and 1s, 2s, and 2p for carbon and oxygen) and consists of least-squares Gaussian representations of Slater-type orbitals (STO-NG).<sup>10</sup> In this work, each STO is replaced by a sum of three Gaussian functions. The exponents used by the 2s and 2p orbitals on the same atom are identical, and the standard scale factors proposed for this basis are used.<sup>10</sup> Both the STO-3G and STO-4G basis sets have been used quite successfully in previous

studies of ground and excited states.<sup>7,11,12</sup> For reasons of economy of computer time, the STO-3G basis set was used for this study of the excited states of ketene. All calculations were performed in double precision on an IBM 360/50 computer.

**Geometry Optimization.** The ground state geometry of ketene was restricted to  $C_s$  symmetry, and the C-H bond length and H-C-H angle were held fixed at their experimental values of 1.079 Å and 122.3°, respectively.<sup>13</sup> The angle  $\omega$  was defined as the angle between the C-C and C-O bonds for nonplanar  $C_s$  symmetry, while  $\theta$  was defined as the angle between the C-C and C-O bonds for planar  $C_s$  ketene. The calculated ground state has  $\omega = \theta = 180^\circ$ , so that ketene has  $C_{2v}$  symmetry in this state. Variation of the C-C and C-O bond lengths was carried out until a minimum energy structure was obtained with respect to a  $\pm 0.01$  Å change in these parameters.

In the excited states, the C-H bond length and the H-C-H angle were again held fixed at their ground state values, and the molecule was restricted to either planar or nonplanar  $C_s$  symmetry. The optimum values of the C-C and C-O bonds and of the angle  $\omega$  (or  $\theta$ ) were obtained by an interpolation technique. First, it was assumed that the potential curve for the energy as a function of each geometrical parameter can be represented near the minimum energy point by a parabola. With two geometrical parameters held constant, the third parameter was then allowed to assume three values  $x_1, x_2, x_3$  ( $x_1 < x_2 < x_3$ ) and the respective energies  $\epsilon_1, \epsilon_2$ , and  $\epsilon_3$  for the excited states were computed. The interval  $\Delta x = x_3 - x_2 = x_2 - x_1$  was chosen as 0.03 Å for bond distances and 3° for bond angles. An optimized value of the variable was obtained by fitting a parabola through the points corresponding to  $\epsilon_1, \epsilon_2, \epsilon_3$ , and finding the value  $\hat{x}$  at which the minimum energy  $\hat{\epsilon}$  occurred. The optimized value  $\hat{x}$  was used only if  $x_1 \leq \hat{x} \leq x_3$ ; otherwise, further points were calculated until this condition was satisfied.  $\hat{x}$  was then used as a fixed parameter while a second parameter was varied. The C-C and C-O bonds and the angle  $\omega$  (or  $\theta$ ) were optimized cyclicly and independently for each excited state. The interpolation process was continued until at the last cycle, the optimized value  $\hat{x}$  for each parameter was within  $\Delta x$  of the optimized value from the preceding cycle. The excited state geometries and energies reported here are those which correspond to that point on the potential surface at which the optimized values of the three geometrical parameters were found.

**Interpolation Error Analysis.** Because the energies of the various excited states are of such importance, it is necessary to analyze the error in the energy of each state which may result from interpolation. From the theory of interpolation it is well known that a function  $f(x)$  can be replaced by an  $n$ th degree algebraic polynomial. In this study, a parabola has been used as the interpolation polynomial, and Newton's forward interpolation formula for equally spaced arguments has been employed to obtain an expression for the resulting inter-

(11) M. D. Newton, W. A. Lathan, W. J. Hehre, and J. A. Pople, *ibid.*, **52**, 4064 (1970).

(12) W. A. Lathan, W. J. Hehre, and J. A. Pople, *J. Amer. Chem. Soc.*, **93**, 808 (1971).

(13) G. Herzberg, "Electronic Spectra of Polyatomic Molecules," Van Nostrand, Princeton, N. J., 1966.

(8) C. C. J. Roothaan, *Rev. Mod. Phys.*, **23**, 69 (1951).

(9) J. E. Del Bene, R. Ditchfield, and J. A. Pople, *J. Chem. Phys.*, **55**, 2236 (1971).

(10) W. J. Hehre, R. F. Stewart, and J. A. Pople, *ibid.*, **51**, 2657 (1969).

**Table I.** Interpolation Errors in Excited State Energies (eV)

Geometrical parameter	$^1A''$	$^3A''$	$^3A'$
$R(C-O)$	0.001	0.001	0.002
$R(C-C)$	0.002	0.001	0.001
$\omega$ (or $\theta^a$ )	(0.002)	(0.001)	0.001

<sup>a</sup>  $\theta$  values are given in parentheses.

**Table II.** Geometries and Excitation Energies for Low-Energy Electronic States of Ketene<sup>a</sup>

State	$R(C-O)$	$R(C-C)$	$\omega$ (or $\theta^b$ )	$\Delta E_{0-0}$	$\Delta E_{\lambda_{max}}$	Experimental <sup>c</sup>	
						$\Delta E_{\lambda_{max}}$	Band width
$^1A_1$	1.18	1.30	180				
$^1A''$	1.24	1.37	(130)	3.34	4.30	3.84	3.34-4.77
$^3A''$	1.26	1.36	(127)	2.46	3.71	3.35	2.62-3.35
$^3A'$	1.20	1.54	123	1.71	4.88		

<sup>a</sup> Energies in electron volts, bond lengths in ångströms, angles in degrees. <sup>b</sup>  $\theta$  values are given in parentheses. <sup>c</sup> Experimental data taken from ref 3 and 4.

polation error.<sup>14</sup> The interpolation error can be evaluated at the interpolated energy minimum of the parabola, and an upper bound on the error can easily be obtained providing  $x_1 \leq \hat{x} \leq x_3$ . Upper bounds on the interpolation errors have been calculated and are reported in Table I. They should be compared with the 0-0 energies which are given in Table II. Such a comparison indicates that the interpolation errors are significantly less than the energy differences among the low-energy electronic states of ketene. Therefore, interpolation errors should not lead to any gross errors in conclusions drawn about the structures and energies of these states.

## Results and Discussion

Optimization of the geometrical parameters for the ground state of ketene produced a structure having  $C_{2v}$  symmetry, with a C-C bond of 1.30 Å and a C-O bond of 1.18 Å, as illustrated in Figure 1. This structure compares quite well with the experimentally determined structure in which C-C and C-O bonds are given as 1.315 and 1.16 Å, respectively, although only the total C-C plus C-O length of 2.475 Å has been accurately determined.<sup>13</sup> The Milliken gross atomic populations<sup>15</sup> given in Table III suggest that both the meth-

**Table III.** Mulliken Gross Atomic Populations

	$^1A_1$	$^1A''$	$^3A''$	$^3A'$
O <sub>1</sub>	8.188	8.080	8.017	8.152
C <sub>2</sub>	5.739	6.221	6.235	5.921
C <sub>3</sub>	6.246	5.824	5.876	6.083
H <sub>4</sub>	0.914	0.936	0.935	0.922
H <sub>5</sub>	0.914	0.939	0.936	0.922

ylene carbon and the oxygen atom bear partial negative charges in the ground state.

In the ground state, the highest occupied orbital has  $b_1$  symmetry ( $\pi$ ) and is principally a bonding orbital between the carbon atoms and somewhat antibonding in the C-O group. The lowest energy virtual orbital has  $b_2$  symmetry ( $\pi'$ ) and is an antibonding orbital

(14) K. S. Kunz, "Numerical Analysis," McGraw-Hill, New York, N. Y., 1957.

(15) R. S. Mulliken, *J. Chem. Phys.*, **3**, 1833 (1955).

in the C-O group.<sup>16</sup> Above this lies a  $b_1$  orbital which is antibonding with respect to C-C and C-O. Configurations in which these orbitals are singly occupied are the principal contributors to the low-energy vertical excited states of ketene. The results of the CI calculations for the lowest excited singlet and the two low-energy triplet states at the ground state geometry are

given in Table II. These vertical excitation energies are to be compared with experimental energies corresponding to the maxima of the Franck-Condon envelopes ( $\lambda_{max}$  values).

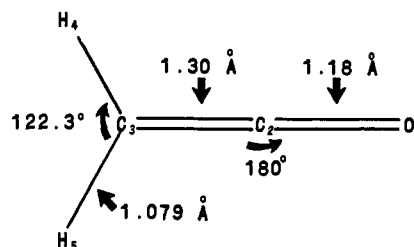


Figure 1. The ground state geometry of ketene.

The lowest energy vertical excited singlet state of ketene arises from a  $b_1 \rightarrow b_2^*$  ( $\pi \rightarrow \pi'^*$ ) transition. This transition gives rise to a configuration which is the only significantly large contributor to the  $^1A_2$  state, at 4.30 eV above the ground state. In point group  $C_{2v}$ , the  $^1A_2 \leftarrow ^1A_1$  transition is symmetry forbidden. Corresponding to the  $^1A_2$  state is the  $^3A_2$  state which arises primarily from the same  $b_1 \rightarrow b_2^*$  transition. At the ground state geometry, the  $^3A_2$  state is the lowest excited state of ketene, having an energy 3.71 eV above the ground state. Above the  $^3A_2$  and  $^1A_2$  states comes the  $^3A_1$  state. The vertical excitation energy for the  $^3A_1 \leftarrow ^1A_1$  excitation is 4.88 eV. The  $^3A_1$  state is also described almost entirely by a single configuration, this one resulting from a  $b_1 \rightarrow b_1^*$  ( $\pi \rightarrow \pi^*$ ) transition.

Now that the energies of the low-lying vertical excited states of ketene have been calculated and the configurations giving rise to these states identified, it is important that the equilibrium geometries and energies of these states be determined. The calculated energy difference between the ground state and an optimized excited state of a molecule is the theoretical  $T_0$  value. Calculated  $T_0$  values are often compared with experimental  $T_0$  values, which are energy differences between zeroth vibrational levels of two electronic states (the "0-0" band). Fortunately, differences between  $T_0$

(16) In  $C_{2v}$  symmetry the orbitals designated  $\pi'$  lie in the molecular plane parallel to the  $y$  axis.

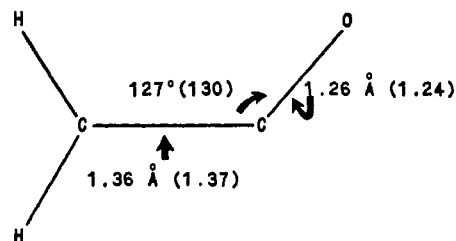


Figure 2. The geometry of the  ${}^3A''$  and  ${}^1A''$  states of ketene. Values in parentheses are the singlet state values.

and  $T_0$  are generally small. Therefore, in the discussion which follows, differences in the zero-point energies of two electronic states will be ignored, and  $T_e$  values will be used as 0-0 energies.

In the search for the equilibrium structures of the excited states of ketene, the molecular geometries were restricted to either planar or nonplanar  $C_s$  symmetry. It was observed that vertical states arising from the  $b_1 \rightarrow b_2^*$  transition become planar excited states in which the C-O bond is bent in the plane of the molecule. In planar  $C_s$  ketene, the  $b_1$  and  $b_2$  orbitals of the  $C_{2v}$  ground state become  $a''$  and  $a'$ , respectively, with the  $a'' \rightarrow a'^*$  transition giving rise to  $A''$  states. On the other hand, the  ${}^3A_1$  state becomes an excited state with an equilibrium structure in which the C-O bond bends out of the plane of the  $CH_2$  group, giving a molecular geometry with nonplanar  $C_s$  symmetry. The  $b_1$  orbital in  $C_{2v}$  symmetry becomes an  $a'$  orbital in nonplanar  $C_s$  symmetry, and the transition  $a' \rightarrow a'^*$  leads to an excited  ${}^3A'$  state. The optimized geometries for the lowest excited singlet state and the two low-energy triplet states of ketene will now be presented and discussed in turn.

The optimized geometries of the excited states of ketene are given in Table II and illustrated in Figures 2 and 3. Also given in Table II are the calculated values for the 0-0 excitation energies and the available experimental data. The lowest singlet excited state of ketene has  ${}^1A''$  symmetry in point group  $C_s$  (planar). This state arises primarily from a single configuration obtained from the  $a'' \rightarrow a'^*$  transition, corresponding to  $b_1 \rightarrow b_2^*$  in the  $C_{2v}$  geometry. Both the C-C and C-O bonds are lengthened in this state by about the same amount, to 1.37 and 1.24 Å, respectively. The gross atomic populations in this state are considerably different from the ground state populations, as shown in Table III. In particular, the negatively charged methylene carbon of the ground state becomes positively charged in the excited state, while the carbonyl carbon, positively charged in the ground state, becomes negatively charged in the excited state. In the  ${}^1A''$  state, electron density is removed from the  $\pi$  system and increased in the molecular plane, primarily around the carbonyl carbon.

Corresponding to the  ${}^1A''$  state is the  ${}^3A''$  state which lies 0.88 eV below it. The geometry of this state is quite similar to that of the  ${}^1A''$  state, with a C-C bond of 1.36 Å, a C-O bond of 1.26 Å, and an angle  $\theta = 127^\circ$ . The general features of the electronic distribution in this state are the same as in the  ${}^1A''$  state, as indicated by a comparison of the Mulliken gross populations. However, the  ${}^3A''$  state is not the lowest triplet state of ketene. Rather, the lowest triplet is

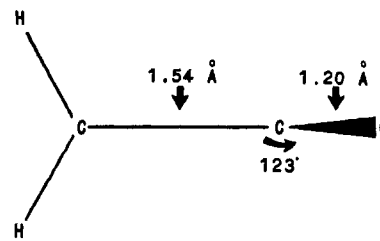


Figure 3. The geometry of the  ${}^3A'$  state of ketene.

related to the  ${}^3A_1$  state which was described above by a single configuration arising from a  $\pi \rightarrow \pi^*$  ( $b_1 \rightarrow b_1^*$ ) transition. Optimization of the  ${}^3A_1$  state led to the  ${}^3A'$  state in molecular point group  $C_s$  (nonplanar). At this geometry, the  $a'$  orbital ( $b_1$  in  $C_{2v}$ ) is the lowest energy virtual orbital, and the transition  $a' \rightarrow a'^*$  produces the single configuration which well describes the  ${}^3A'$  state. This state has an energy 1.71 eV above the ground state and is characterized by a very long C-C bond of 1.54 Å and a C-O bond strongly bent out of the  $CH_2$  plane. There is little change in the length of the C-O bond in going from the  ${}^1A_1$  to the  ${}^3A'$  state. In contrast to the ground state and the other low-energy excited states of ketene, there is comparatively little buildup of charge on the carbon atoms in the  ${}^3A'$  state, as shown by the Mulliken gross atomic populations given in Table III.

**Spectroscopy and Photochemistry.** Dixon and Kirby<sup>3</sup> have studied the long-wavelength absorption spectrum of ketene where they observed an electronic transition between 4735 and 3700 Å (2.62–3.35 eV). They assigned this band to a  ${}^3A_2 \leftarrow {}^1A_1$  transition. McGlynn, *et al.*,<sup>4</sup> have also observed this band and have suggested that it may arise from two different singlet-triplet transitions. Recently, Laufer and Keller<sup>5</sup> have proposed that this band is really part of a higher energy band and that no spin-forbidden transitions occur in ketene. The calculated energies for the  ${}^3A''$  ( ${}^3A_2$ )  $\leftarrow$   ${}^1A_1$  excitation are in reasonable agreement with the energies given by Dixon and Kirby for the singlet-triplet transition and therefore support their assignment for this band.

Following the band between 4735 and 3700 Å is a second weak, diffuse band which extends from 3706 to 2601 Å (3.34–4.77 eV). There is agreement among various studies that this transition is due to a  ${}^1A_2 \leftarrow {}^1A_1$  excitation and that the transition giving rise to the  ${}^1A_2$  state is analogous to the  $n \rightarrow \pi^*$  transition of formaldehyde.<sup>3,4,13</sup> The data presented here support the assignment of this band to a  ${}^1A''$  ( ${}^1A_2$ )  $\leftarrow$   ${}^1A_1$  excitation, although the transition giving rise to this band is not an  $n \rightarrow \pi^*$  transition. This point will be discussed in more detail below. The weak intensity of this band is due to the fact that the  ${}^1A_2 \leftarrow {}^1A_1$  transition in point group  $C_{2v}$  is symmetry forbidden.

McGlynn<sup>4</sup> has noted that there should be two low-energy singlet-triplet transitions in ketene, both of which may contribute to the first absorption band between 4735 and 3700 Å. However, the  $\lambda_{max}$  value corresponding to excitation to the  ${}^3A_1$  state indicates that the  ${}^3A'$  ( ${}^3A_1$ )  $\leftarrow$   ${}^1A_1$  transition may contribute to the band between 3706 and 2601 Å instead, since the Franck-Condon accessible region for this excitation is of a rather high energy. Because of the large energy

difference between the  $\lambda_{\text{max}}$  and 0-0 values, no 0-0 band for excitation to the relaxed  $^3A'$  state is likely to occur in the spectrum.

Since the transition giving rise to the first singlet absorption band in ketene has frequently been likened to the  $n \rightarrow \pi^*$  transition in formaldehyde, a comparison of the lowest excited singlet states in these two molecules is in order. At the ketene ground state geometry, the  $^1A_2$  state arises from a  $b_1 \rightarrow b_2^*$  transition in which an electron is removed from a  $\pi$  orbital and placed in a  $\pi'$  orbital which lies in the molecular plane. On the other hand, the  $^1A_2$  state of formaldehyde arises from a  $b_2 \rightarrow b_1^*$  transition, in which an electron is removed from the molecular plane and placed in a  $\pi$  orbital. Optimization of the  $^1A_2$  excited state of ketene leads to a state of  $^1A''$  symmetry in molecular point group  $C_s$  in which the molecule is planar. In this state, there is a considerable increase in the electron density at the carbonyl carbon atom and only a slight decrease in electron density at the oxygen, which still bears a small negative charge. Optimization of the  $^1A_2$  excited state of formaldehyde also led to a  $^1A''$  state but with nonplanar molecular  $C_s$  symmetry. In the  $^1A''$  state, the C-O bond bends in the plane defined by the  $\text{CH}_2$  group in ketene and out of this plane in formaldehyde. Moreover, in going from the  $^1A_1$  state of formaldehyde to the  $^1A''$  state, the oxygen atom which was negatively charged in the ground state becomes quite positively charged in the excited state, the gross atomic population changing from 8.158 to 7.797 e. The carbonyl carbon, which was about neutral in the ground state with a gross atomic population of 5.981 e, acquires a large negative charge in the excited state with a population of 6.460 e. Thus, the lowest excited  $^1A''$  state of ketene differs from the  $^1A''$  state of formaldehyde in the nature of the transitions which give rise to these states, and in molecular geometry and electronic structure. Hence, the  $^1A''$  state of ketene cannot be adequately described nor understood by analogy with the  $^1A''$  state of formaldehyde.<sup>17</sup>

For a complete description of the photochemistry of ketene, it is necessary to obtain information about the nature of the potential surfaces for the ground and excited states as a function of all geometrical parameters. While such a description is theoretically possible to obtain, it is impractical because of the amount of computer time required. However, it is possible to obtain some information about these surfaces by examining the potential curves for these states with respect to changes in a particular geometrical parameter. The curves as a function of the C-C bond length are of special interest, since it is known that ketene dissociates into  $\text{CH}_2$  and  $\text{CO}$ . Such a set of curves is reproduced in Figure 4.

In this figure, the points labeled  $^3A_1$ ,  $^3A_2$ , and  $^1A_2$  at a C-C bond distance of 1.30 Å correspond to the vertical excitation energies to these respective states. At the right hand side of Figure 4 at  $R = \infty$ , the calculated energies of the dissociation products  $\text{CH}_2$  ( $^3B_1$ ) and  $\text{CO}$ , and  $\text{CH}_2$  ( $^1B_1$ ) and  $\text{CO}$ , are indicated. For these calculations, the geometry of  $\text{CH}_2$  was taken from the  $\text{CH}_2$  geometry in the ground state of ketene.<sup>18</sup>

(17) The data quoted here for formaldehyde were obtained in the study reported in ref 7.

(18) It is interesting to note that the calculated energies for the  $^3B_1$  and  $^1B_1$  states of  $\text{CH}_2$  at the geometry of the  $\text{CH}_2$  group in the ground

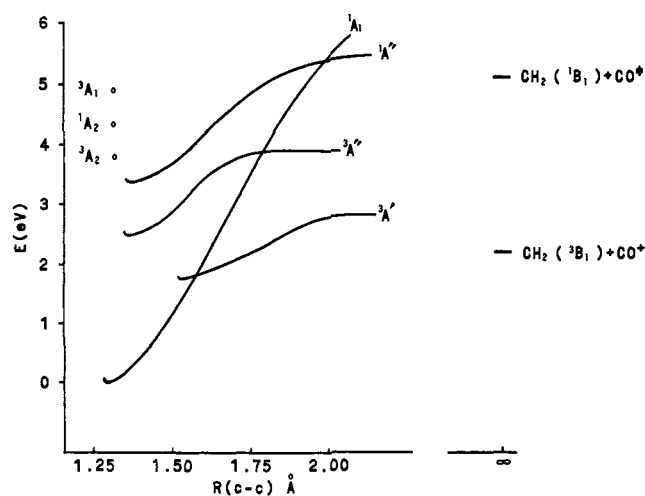


Figure 4. Potential curves for low-energy states of ketene as a function of the C-C bond length. The energies are given as  $\Delta E$  values relative to the ground state energy.  $\text{CO}^+$  and  $\text{CO}^\pm$  represent vibrationally excited CO molecules. See text for a further explanation of the figure.

The energies of  $^3B_1$  and  $^1B_1$   $\text{CH}_2$  were calculated from CI wave functions which included nine configurations. The energies for the closed shell CO molecules were obtained from single-determinant functions for CO with bond lengths of 1.20 and 1.24 Å, the C-O distances in the  $^3A'$  and  $^1A''$  states of ketene, respectively.

For each curve in Figure 4, the C-H bond distance and the H-C-H angle were held constant as before, and the values of the C-O bond length and the angle  $\omega$  (or  $\theta$ ) were fixed at the equilibrium values for each state. The  $^1A_1$  curve was produced from single-determinant wave functions, while curves for the open shell states were obtained from CI calculations including 36 singly excited configurations constructed from the SCF orbitals for the closed shell states at the appropriate geometries. Obviously, there are correlation energy errors in these curves, and such errors may be expected to vary in each state as the C-C bond length is changed. Moreover, the dissociation of ketene into  $\text{CH}_2$  and  $\text{CO}$  probably does not follow any curve in which all geometrical parameters except one are held constant. Nevertheless, these curves should reflect the general behavior of the low-energy states of ketene as a function of the C-C bond length, and some general observations can be made on the basis of Figure 4.

It was noted above that because there is a large change in the geometry of ketene in going from the  $^1A_1$  to the relaxed  $^3A'$  state, the vertical excitation energy is significantly higher than the calculated 0-0 excitation energy for the  $^3A'(^3A_1) \leftarrow ^1A_1$  transition. Figure 4 suggests that excitation from the ground state to the Franck-Condon accessible region of the  $^3A'$  state leads to dissociation, since the energy required for the  $^3A_1 \leftarrow ^1A_1$  transition is greater than the dissociation limit of the  $^3A'$  state. Therefore, the relaxed  $^3A'$  state may not be formed by direct absorption of energy from the ground state. It may, however, be formed from other low-energy states *via* an internal nonradiative process.

state of ketene are close to energies of geometry-optimized radicals in these states. In both states, the potential curves for changes in the H-C-H angle are shallow. See, for example, J. E. Del Bene, *Chem. Phys. Lett.*, **9**, 68 (1970), and references cited therein.

An analysis of Figure 4 also suggests that the  $^3A'$  state of ketene may dissociate into triplet  $CH_2$  ( $^3B_1$ ) and a vibrationally excited CO molecule. It is also reasonable to expect that the  $^3A''$  state dissociates to the same products, especially since it is known experimentally that the next excited triplet state of  $CH_2$  is approximately 8.7 eV above the  $^3B_1$  state,<sup>13</sup> and would not appear to be accessible from either of the low-energy triplet states of ketene. The dissociation of the  $^1A''$  state to  $CH_2$  ( $^1B_1$ ) and vibrationally excited CO is also apparent from Figure 4. This does not preclude the possibility of other excited singlet states of ketene dissociating to the same products. It might even be expected that the singlet state corresponding to the vertical  $^3A_1$  state would be of importance in the photochemistry of this molecule.<sup>19</sup>

It is known experimentally that irradiation of ketene between 2700 and 2900 Å (4.29–4.59 eV) produces almost exclusively singlet  $CH_2$ .<sup>20</sup> Undoubtedly excitation to the  $^1A''$  state is important in this process. Moreover, the almost exclusive production of singlet  $CH_2$  suggests that only a few molecules are excited to the  $^3A_1$  ( $^3A'$ ) state at these wavelengths. At longer wavelengths, irradiation of ketene produces an increasing amount of triplet  $CH_2$ . At 3660 Å (3.39 eV) the ratio of triplet to singlet  $CH_2$  is 0.4, while between 3460 and 3820 Å (3.25–3.58 eV) the ratio becomes greater than 0.5.<sup>20</sup> These data suggest that the  $^3A''$  state does indeed dissociate to triplet  $CH_2$ . However,

(19) No calculations for the excited  $^1A_1$  state have been reported here since it has already been demonstrated in ref 9 that a larger basis set than that used in this work is necessary to obtain even a moderate approximation to singlet  $\pi \rightarrow \pi^*$  excitation energies.

(20) J. W. Calvert and J. N. Pitts, "Photochemistry," Wiley, New York, N. Y., 1967.

the fact that singlet  $CH_2$  is also formed at longer wavelengths indicates that the dissociation energy for the  $^1A''$  state may be lower than indicated in Figure 4.

## Conclusions

On the basis of the calculations performed in this study, it is possible to draw the following tentative conclusions. 1. The two low-energy bands of the ketene spectrum arise from  $^3A''(^3A_2) \leftarrow ^1A_1$  and  $^1A''(^1A_2) \leftarrow ^1A_1$  excitations, respectively. The transition giving rise to these states is not, however, analogous to the low-energy transition observed in formaldehyde. 2. In the  $^3A''$  and  $^1A''$  states, ketene has planar molecular  $C_s$  symmetry, in which the C–O bond is strongly bent in the molecular plane, and the C–C and C–O bonds are lengthened. 3. The lowest energy triplet state of ketene is of  $^3A'$  symmetry in point group  $C_s$  (nonplanar) and is characterized by a very long C–C bond. For large C–C bond distances, this state is the lowest energy state in ketene. Because of the difference between the vertical excitation energy and the 0–0 energy for the  $^3A'(^3A_1) \leftarrow ^1A_1$  excitation, the relaxed  $^3A'$  state may not be formed directly by absorption of energy from the ground state. 4. Dissociation may occur from the  $^3A'$  and  $^3A''$  states of ketene yielding  $CH_2$  ( $^3B_1$ ) and vibrationally excited CO. The  $^1A''$  state may also dissociate, giving  $CH_2$  ( $^1B_1$ ) and CO.

**Acknowledgments.** Thanks are due to Dr. Ronald Jonas and the staff of the Youngstown State University Computer Center for their generous and helpful cooperation in this project, to Dr. Howard Mettee for many valuable discussions on photochemistry, and to Mr. Gus Mavrigian for assistance with the error analysis.

## Molecular Orbital Theory of E2 Reactions and Nuclear Magnetic Resonance Spin–Spin Coupling in Ethane-Like Molecules<sup>1</sup>

John P. Lowe

Contribution from the Department of Chemistry,  
The Pennsylvania State University, University Park, Pennsylvania 16802.  
Received October 19, 1971

**Abstract:** Molecular orbital calculations of syn and anti modes of E2 reactions are analyzed in terms of current reactivity theories. The roles of charge polarization and charge transfer are analyzed. The effects of charge transfer appear to be only partly understandable in terms of the lowest empty MO of the substrate. The tendency for syn eliminations to proceed through a more E1cb-like transition state is shown to result in part from charge polarization produced by negative base. The torsional angle dependence of vicinal nmr spin–spin coupling in ethane is calculated and rationalized in terms of delocalized MO's. This phenomenon is shown to be closely related to the nature of charge delocalization into substituted ethanes by attacking base. As a result, there is good reason to expect strong nmr spin coupling between sites which are strongly coupled in E2 reactions.

When staggered haloethane undergoes base-assisted bimolecular elimination (E2 reaction), the base attacks and removes the proton trans planar from halogen X (anti elimination),<sup>2,3</sup> charge is transferred to the

departing halide, the two carbons become  $sp^2$  hybridized, and a  $\pi$  bond is formed. These processes proceed more or less concurrently, and the fact that, under anti attack, the incipient  $\pi$  lobes on the  $\alpha$  and  $\beta$

(1) Acknowledgment is made to the donors of the Petroleum Research Fund, administered by the American Chemical Society, for support of this research.

(2) J. F. Bunnett, *Surv. Progr. Chem.*, **5**, 53 (1969).

(3) C. K. Ingold, "Structure and Mechanism in Organic Chemistry," 2nd ed, Cornell University Press, Ithaca, N. Y., 1969, Chapter 9.